ISSN 1075-7015, Geology of Ore Deposits, 2020, Vol. 62, No. 7, pp. 618–628. © Pleiades Publishing, Ltd., 2020.
Russian Text © The Author(s), 2019, published in Zapiski Rossiiskogo Mineralogicheskogo Obshchestva, 2019, No. 5, pp. 74–88.

MINERALS AND MINERAL PARAGENESES

The Mineral Composition of Paleoproterozoic Metamorphosed Massive Sulfide Ores in the Kola Region (A Case Study of the Bragino Ore Occurrence, Southern Pechenga)

A. A. Kompanchenko[a], *, A. V. Voloshin[a], and A. V. Bazai[a]

[a]*Geological Institute, Kola Science Centre, Russian Academy of Sciences, Apatity, 184209 Russia*

**e-mail: komp-alena@yandex.ru*

Received April 9, 2019; revised May 18, 2019; accepted June 13, 2019

Abstract—Many massive sulfide ore occurrences and deposits in the Kola region are located within the Paleoproterozoic Pechenga–Imandra–Varzuga rift belt (2.5–1.7 Ga). They are hosted by volcanosedimentary complexes of the South Pechenga (Bragino ore occurrence) and western Imandra–Varzuga structural zones (Pirrotinovoe Ushchel'e deposit, Tahtarvumchorr ore occurrence, etc.). The age of the massive sulfide ore was estimated at ca. 1.9 Ga. The ores and their host complexes underwent amphibolite-facies metamorphism, which accounts for their specific mineral composition. The types of ores in the Bragino ore occurrence are discussed, the mineral assemblages are listed, and the major ore minerals, that is, pyrrhotite, pyrite, sphalerite, marcasite, etc., are characterized.

Keywords: massive sulfide ores, pyrite, pyrrhotite, Paleoproterozoic, Kola region

DOI: 10.1134/S1075701520070077

Massive sulfide ore occurrences and deposits in the Kola region are confined to the Pechenga–Imandra–Varzuga (PIV) Paleoproterozoic rift belt, which developed in the interval of 2.5–1.7 Ga (Melezhik and Sturt, 1994; *Rannii dokembrii* ..., 2005; *Reading* ..., 2013; Mints et al., 2015). They are hosted by the volcanosedimentary complexes of the South Pechenga structural zone (SPSZ, Bragino ore occurrence) and in the western part of the Imandra–Varzuga structural zone (also referred to as Cis-Khibiny), at the contact with the Khibiny alkaline massif (Pirrotinovoe Ushchel'e, also referred to as the Pyrrhotite Ravine; Tahtarvumchorr, etc.).

The Bragino massive sulfide ore occurrence was discovered in the metavolcanic rocks of the Mennel Formation of the Porojarvi Group (Fig. 1). The composition of these rocks corresponds to basalts, subalkaline basalts, picrobasalts, and picrites (Skuf'in and Theart, 2005; Skuf'in et al., 2009). The Mennel volcanics are depleted in K, Sr, Rb, Ta, Zr, Hf, Ti, and light and heavy rare-earth elements and are enriched in Ba, Th, and Nb. In terms of the specific features of their composition, they are very similar to the low-alkali, iron- and magnesium-rich mid-oceanic ridge basalts (MORB) (Skuf'in and Theart, 2005). The estimated ages of picrites of the Mennel Formation (1865 ± 58 Ma, Rb–Sr method (Balashov, 1996); 1894 ± 40 Ma, Sm–Nd method (Skuf'in et al., 2009)) are contemporaneous with the volcanics of the undifferentiated Tominga Group (1870 ± 38 Ma, Rb–Sr method (Mitrofanov et al., 1991)). The SPSZ rocks that host the massive sulfide ores underwent amphibolite-facies metamorphism (Skuf'in and Theart, 2005; Skuf'in et al., 2009). The Mennel volcanics near the Bragino ore occurrence are intruded by minor diorite, porphyry granite, lamprophyre, and syenite bodies of the Bragino Suite and display widespread metasomatic rocks such as quartzites, beresites, listvenites, and albitites (Akhmedov et al., 2004) (Fig. 1).

Based on the published data (Akhmedov et al., 2004) and our field observations, we may conclude that the massive sulfide ore body of the Bragino ore occurrence is a lens that is 5 to 7 m in thickness and probably up to 100 meters in length; it is NW–SE trending and NE-dipping at 70°–75°. It is exposed in several trenches (Fig. 2) but is largely blanketed by Quaternary sediments; therefore, its precise dimensions and relationship with host rocks remain unknown. Thin albitite and quartzite zones were reported in one trench at the contacts of massive sulfide ores with volcanic host rocks.

MATERIALS AND METHODS

Massive sulfide ore minerals were examined under an Axioplan optical microscope in reflected and transmitted polarized light. The mineral morphology and phase and intraphase heterogeneity were studied using a LEO-1450 scanning electron microscope (SEM), equipped with a Bkuker XFlash 5010 energy dispersive

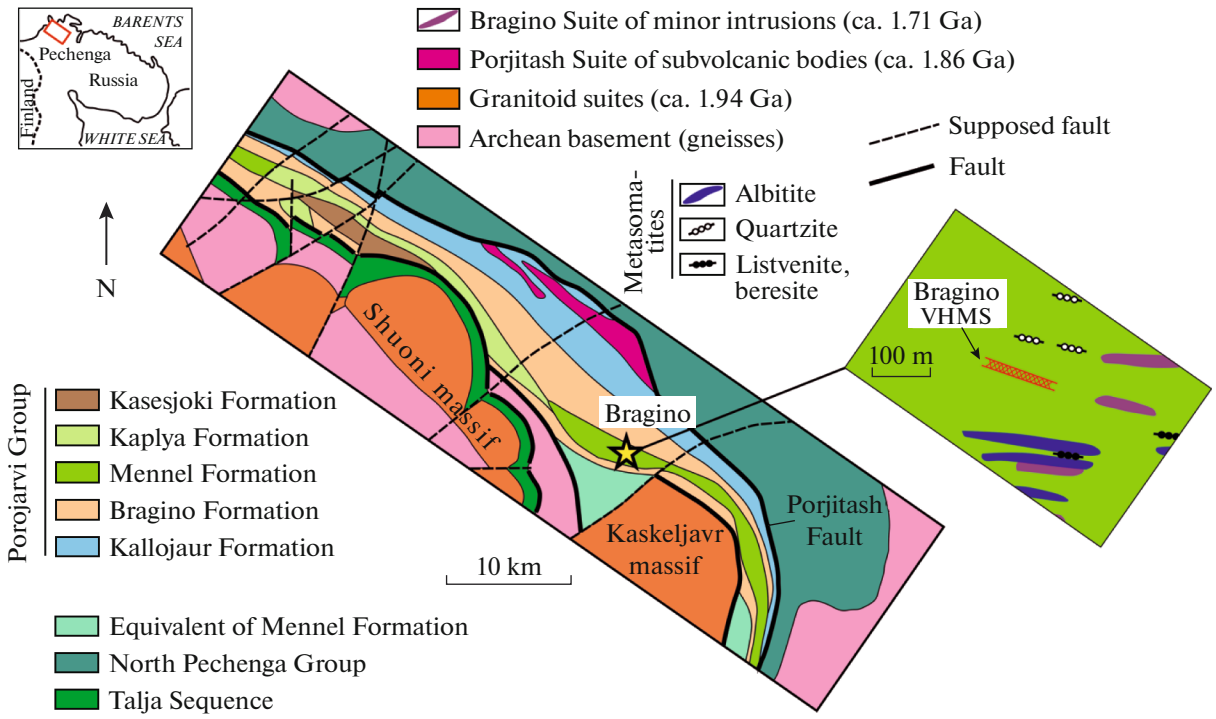

Fig. 1. The geological map of the South Pechenga structural zone and the position of the Bragino ore occurrence (modified after Melezhik and Sturt, 1994; Akhmedov et al., 2004; Skuf'in and Theart, 2005; *Reading* ..., 2013; Kompanchenko et al., 2018).

spectrometer (EDS) (analyst A.V. Bazai, Geological Institute, Kola Science Centre, Russian Academy of Sciences (GI KSC RAS), Apatity, and a Hitachi S-3400N SEM with an Oxford X-Max 20 EDS (analysts N.S. Vlasenko and V.V. Shilovskikh, Geomodel Resource Centre of St. Petersburg State University (SPbSU), St. Petersburg). Chemical analysis of homogeneous mineral grains larger than 20 μm was performed using a Cameca MS-46 electron probe microanalyzer (EPMA) in GI KSC RAS (analyst A.V. Bazai). The mineral microhardness was measured using a PMT-3 device under a load of 50–100 g; X-ray phase analysis was performed using a URS-55 X-ray apparatus (analysts E.A. Selivanova, M.V. Toropova, and M.Yu. Glazunova, GI KSC RAS). In order to reveal the interior structure of pyrite grains, the mineral was etched with concentrated HNO_3 with fluorite powder.

RESULTS

In terms of rock structure, the massive sulfide ores of the Bragino ore occurrence were subdivided into massive, banded, brecciated, and disseminated types. Special attention was given to the massive ores as the most widespread type. The other varieties were encountered mostly in the marginal parts of the orebody.

In terms of mineral composition, massive ores can be subdivided into three types, pyrrhotite type I (mPo-I), pyrrhotite type II (mPo-II), and pyrite (mPy) (Table 1). It can be noted that the massive sulfide ores of the Cis-Khibiny Just Cis-Khibiny or Imandra-Varzuga structure zone are similar to the pyrrhotite type II ores.

The massive pyrrhotite type I ores have been recognized in the central part of the orebody (exposed in trench 8, Fig. 2) and consist of 90–95% sulfides, of which pyrrhotite accounts for 80%. This ore type is characterized by the groundmass of fine grained monoclinic and hexagonal pyrrhotite, which contains coarser grained hexagonal pyrrhotite veinlets (Figs. 3 and 4a, 4b). Other sulfides are marcasite, chalcopyrite, and less frequent molybdenite and galena (Table 2, Fig. 4). Molybdenite occurs as thin (a few μm) flakes up to 10–15 μm in length. It is usually associated with the intergrowths of the minerals of crichtonite group and rutile (Fig. 4i) and scarcely occurs independently. Galena was encountered as extra fine (up to 10 μm) xenomorphic segregations in the pyrrhotite matrix.

The rare and accessory minerals are represented by vanadium and vanadium-bearing minerals such as coulsonite, rutile, crichtonite, senaite, phlogopite, clinochlore, and talc (Figs. 4d–4i). The phlogopite–clinochlore association was encountered in massive pyrrhotite type I ores exclusively (Table 2). Coulsonite in this ore type occurs as crystals with octahedral habits and as intergrowths up to 500 μm across; in this case, its microhardness is two times higher than the described one (743 kg/mm^2 against 338 kg/mm^2, according to (Karpov et al., 2013)). The chemical composition of

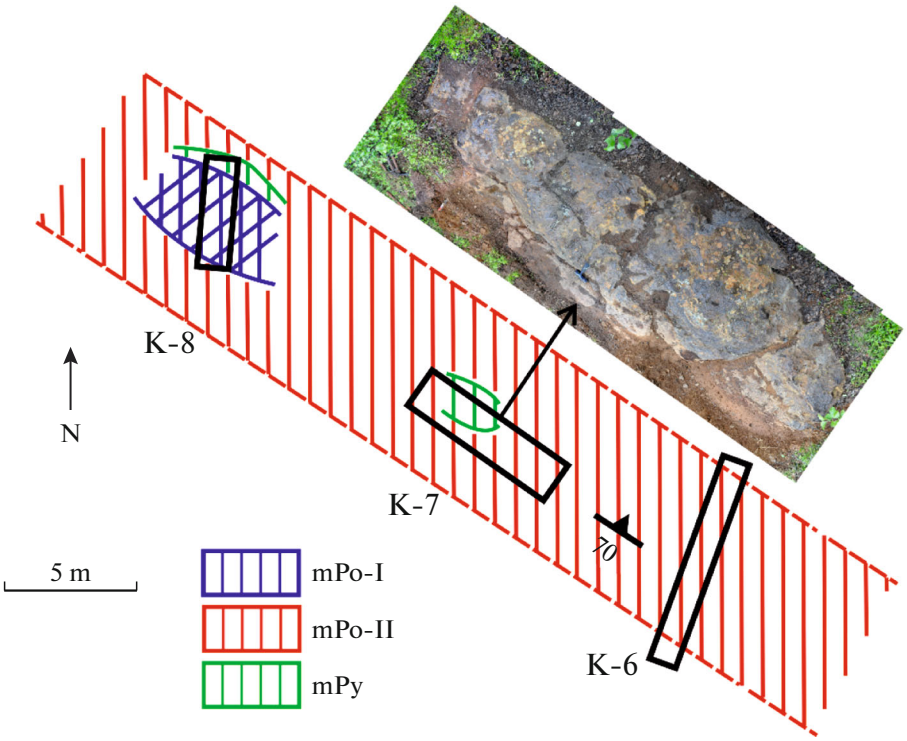

Fig. 2. The distribution of various ore types at the Bragino occurrence (modified after Akhmedov et al., 2004).

the mineral is characterized by a high chromium content (near 20% Cr_2O_3).

The pyrrhotite mass in the oxidation zone of this ore type is extensively replaced by a pyrite–marcasite aggregate with a bird's-eye texture (Figs. 4c, 4g, 4h), which is overprinted by hydrous iron oxides, that is, goethite and lepidocrocite, and less frequent iron sulfates, that is, melanterite and rozenite (Kompanchenko et al., 2017b).

In terms of chemical composition, the mPo-I ores are characterized by the lowest (among all recognized ore types) Au, Cu, and V grades, which are similar to

Table 1. The massive sulfide ore types at the Bragino ore occurrence

Composition/Ore type	mPo-I	mPo-II	mPy
Sulfide content, vol %	90–95	80–85	80–85
Major and minor minerals, vol %	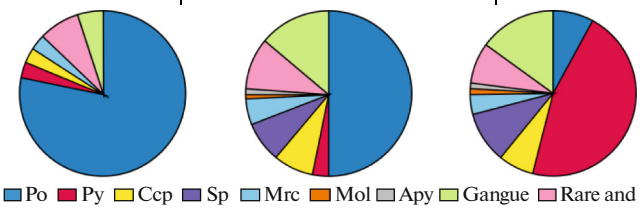		
Noble metal content, g/t	Au 0.10	Au 0.26	Au 0.20
	Ag 2.82	Ag 3.23	Ag 2.57
	Pt n.f.	Pt 0.03	Pt 0.02
Nonferrous metal content, wt %	Cu 0.026	Cu 0.063	Cu 0.084
	Ni 0.071	Ni 0.051	Ni 0.023
	Co 0.004	Co 0.003	Co 0.010
V_2O_5 content, wt %	0.025	0.054	0.047
Quartz–albite vein relics	Absent	Present	Present

Apy—arsenopyrite, Ccp—chalcopyrite, Mol—molybdenite, Mrc—marcasite, Po—pyrrhotite, Py—pyrite; gangue—the main gangue minerals (quartz, albite, and siderite); rare and acc.—rare and accessory minerals. n.f.—not found.

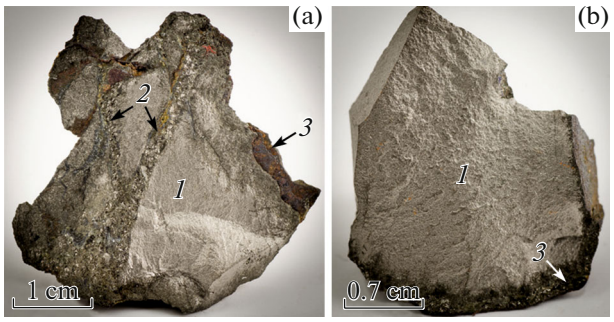

Fig. 3. Samples of type I massive pyrrhotite ore. (*1*) Groundmass, (*2*) hexagonal pyrrhotite veinlets, (*3*) oxidation zone.

the average Ag and Co grades, and the highest Ni grade (Table 1). Platinum was not identified in the ores. The low copper grade is explained by the low extent and extremely small size of chalcopyrite segregations (Fig. 4c). Nickel and cobalt occur as minor elements in pyrrhotite (0.05–0.2 wt % Ni, < 0.1 wt % Co). The high silver grade (Table 2) is surprising, because silver minerals were not identified in this ore type. In all probability, silver, as well as gold, occurs in sulfides as an isomorphous admixture.

The massive pyrrhotite type II ores (Fig. 5) are the most widespread and probably make up more than 80% of the orebody. This ore type is distinguished by the widest mineral diversity (Table 2). As in the massive pyrrhotite type I ores, pyrrhotite is the mineral of primary importance here, but it accounts for only 50% (Table 1). Pyrrhotite is also replaced by the pyrite–marcasite aggregate with a bird's-eye texture (Figs. 6a–6c, 6e–6g), but marcasite proper is also present (Fig. 6d). This ore type displays an abrupt increase in the proportions of other sulfides, that is, sphalerite and chalcopyrite. Sphalerite occurs as large xenomorphic segregations and pockets in close intergrowth with pyrrhotite (Figs. 6g, 6h) or chalcopyrite. Sphalerite was found to contain Fe (up to 10 wt %) and Cd (less than 1 wt %) as minor elements. Sphalerite is characterized by red internal reflex. Chalcopyrite occurs as pockets, veinlets, and minute segregations at pyrrhotite grain boundaries (Figs. 6j, 6k, 6m). Chalcopyrite crystals often display visible twinning. Large chalcopyrite segregations with pyrrhotite and sphalerite inclusions, pierced with minute hisingerite flakes (Fig. 6i) were encountered sporadically. Arsenopyrite occurs occasionally as crystal aggregates up to 500 μm across (Fig. 6k) and, more frequently, as small (up to 20 μm) single crystals. Molybdenite occurs as minute flakes in pyrrhotite or in the complex aggregates of minerals of

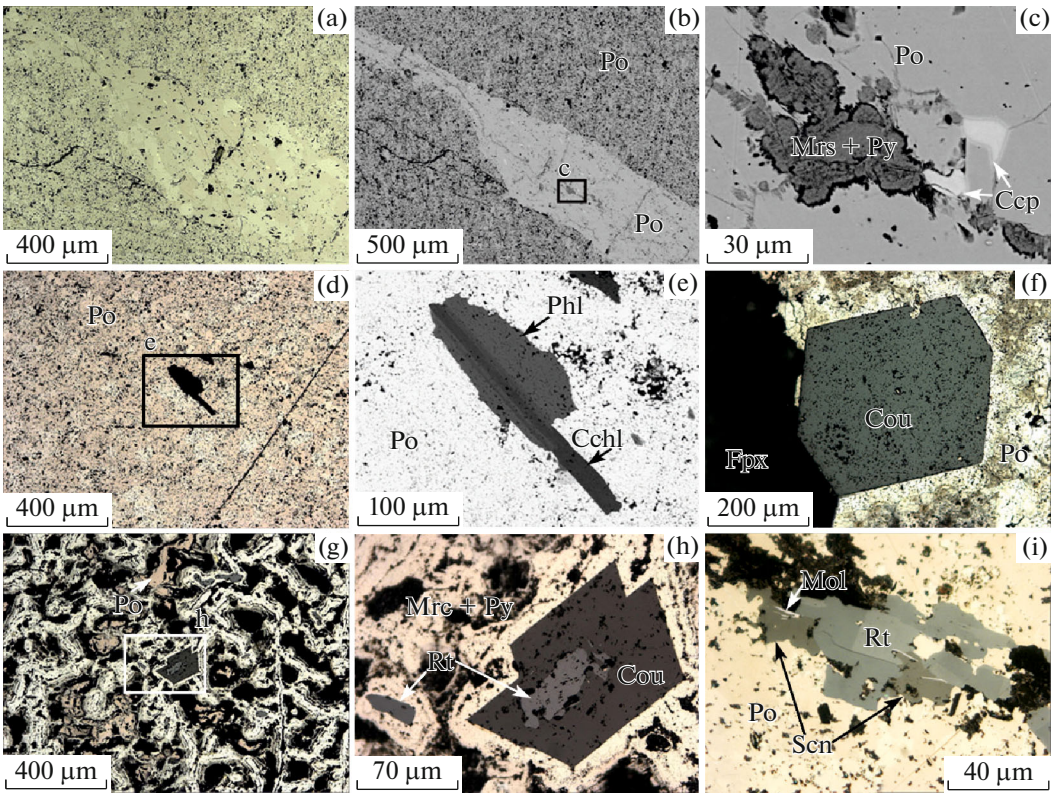

Fig. 4. The major (a–c) and rare (d–i) minerals of type I massive pyrrhotite ores. BSE (b, c, e) and polarized light images (the rest). Cchl, clinochlore; Ccp, chalcopyrite; Cou, coulsonite; Epx, epoxy resin; Mol, molybdenite; Mrc, marcasite; Phl, phlogopite; Po, pyrrhotite; Py, pyrite; Rt, rutile; Sen, senaite.

Table 2. The mineral composition of massive sulfide ores at the Bragino ore occurrence

Mineral	Formula	Ore types		
		mPo-I	mPo-II	mPy
	Native elements			
Gold	Au	–	+	–
	Sulfides, sulfosalts, tellurides			
Pyrrhotite	**Fe_7S_8**	++	++	+
Pyrite	**FeS_2**	+	+	++
Altaite	PbTe	–	+	+
Arsenopyrite	FeAsS	–	+	–
Volynskite	$AgBiTe_2$	–	+	–
Galena	PbS	+	+	+
Hessite	Ag_2Te	–	+	+
Cobaltite	CoAsS	–	+	–
Kotulskite	$Pd(Te,Bi)_{2-x}$ ($x = 0.4$)	–	+	–
Marcasite	**FeS_2**	++	++	+
Molybdenite	MoS_2	+	+	+
Pentlandite	$(Ni,Fe)_9S_8$	–	+	–
Rucklidgeite	$PbBi_2Te_4$	–	+	–
Sphalerite	**ZnS**	–	+	+
Chalcopyrite	**$CuFeS_2$**	+	++	+
	Oxides			
Byrudite*	$(Be, \square)(V^{3+},Ti)_3O_6$	–	+	+
Goethite	α-$Fe^{3+}O(OH)$	+	+	+
Davidite-(Ce)	$Ce(Y,U)Fe_2(Ti,Fe,Cr,V)_{18}(O,OH,F)_{38}$	–	+	–
Davidite-(La)	$La(Y,U)Fe_2(Ti,Fe,Cr,V)_{18}(O,OH,F)_{38}$	–	+	–
Ilmenite	$FeTiO_3$	–	+	+
Quartz	**SiO_2**	+	+	+
Crichtonite	$Sr(Mn,Y,U)Fe_2(Ti,Fe,Cr,V)_{18}(O,OH)_{38}$	–	+	+
Coulsonite	FeV_2O_4	+	+	+
Kyzylkumite	$Ti_2V^3 + O_5(OH)$	–	–	+
Lepidocrocite	γ-$Fe^{3+}O(OH)$	+	+	+
Lindsleyite	$(Ba,Sr)(Zr,Ca)(Fe,Mg)_2(Ti,Cr,Fe)_{18}O_{38}$	–	+	+
Magnetite	$FeFe_2O_4$	–	+	+
Nolanite	$(V^{3+},Fe^{3+},Fe^{2+})_{10}O_{14}(OH)_2$	–	–	+
Rutile	TiO_2	+	+	+
Senaite	$Pb(Mn,Y,U)(Fe,Zn)_2(Ti,Fe,Cr,V)_{18}(O,OH)_{38}$	+	+	+
Tivanite*	$TiV^{3+}O_3(OH)$	–	+	+
Ferberite	$FeWO_4$	–	+	–
Chromite	$FeCr_2O_4$	+	+	–
Schreierite*	$V_2Ti_3O_9$	–	+	–

Table 2. (Contd.)

Mineral	Formula	Ore types		
		mPo-I	mPo-II	mPy
	Carbonates			
Ankerite	$Ca(Fe^{2+},Mg)(CO_3)_2$	–	+	+
Calcite	$Ca(CO_3)$	–	+	+
Siderite	$Fe(CO_3)$	+	+	+
	Sulfates, tungstates			
Barite	$BaSO_4$	–	+	+
Melanterite	$Fe(SO_4) \cdot 7H_2O$	+	+	–
Rozenite	$Fe(SO_4) \cdot 4H_2O$	+	+	–
Scheelite	$Ca(WO_4)$	–	–	+
	Phosphates			
Hydroxylapatite	$Ca_5(PO_4)_3(OH)$	–	+	+
Xenotime-(Y)	$Y(PO_4)$	–	+	+
Monazite-(Nd)	$Nd(PO_4)$	–	+	+
Monazite-(Ce)	$Ce(PO_4)$	–	+	+
	Silicates			
Albite	**$Na(AlSi_3O_8)$**	+	+	+
Hisingerite	$Fe_2Si_2O_5(OH)_4 \cdot 2H_2O$	–	+	+
Jervisite	$NaScSi_2O_6$	–	–	+
Clinochlore	$Mg_5Al(AlSi_3O_{10})(OH)_8$	+	–	–
Microcline	$K(AlSi_3O_8)$	–	+	+
Muscovite	$KAl_2(AlSi_3)O_{10}(OH)_2$	–	+	+
Roscoelite	$KV_2(AlSi_3)O_{10}(OH)_2$	–	+	+
Talc	$Mg_3Si_4O_{10}(OH)_2$	+	–	–
Titanite*	$CaTi(SiO)_4O$	–	+	–
Thortveitite	$Sc_2Si_2O_7$	–	+	+
Phlogopite	$KMg_3(AlSi_3)O_{10}(OH)_2$	+	–	–
Shamosite	$(Fe^{2+},Mg,Al,Fe^{3+})_6(Si,Al)_4(OH,O)_8$	–	+	+

Major minerals are in boldface, ++—Predominant, +—detected in this ore type, *—detected only in quartz–albite vein relics. Dash—not found.

the crichtonite group. Galena is extremely rare. Noble metal mineralization is represented by native gold and tellurides. Native gold was encountered as minute (up to 5 μm) dissemination in pyrrhotite and chalcopyrite (Fig. 6m). In addition, pyrrhotite was found to contain single kotulskite (Fig. 6n) and palladium-carrier cobaltite inclusions. According to the published data, platinum tellurides were also identified in the ores (Akhmedov et al., 2004). The bulk of various tellurides, that is, altaite, hessite, volynskite, and rucklidgeite, is associated with ilmenite–rutile aggregates (Fig. 6o). The representatives of Cr–Sc–V mineralization were also identified among the rare minerals in this ore type as the relics of chromite, coulsonite (Kompanchenko et al., 2017a), V–Sc-bearing minerals of the crichtonite group, etc. (Table 2). The massive pyrrhotite type II ores contain relics of quartz–albite veinlets, which also bear Cr–Sc–V mineralization (Fig. 4).

Type II ores are strongly fractured; the fractures are marked by extensive pyrrhotite replacement by pyrite–marcasite aggregate and goethite emplacement along them (Figs. 6a, 6b). The chemical composition of these ores (Table 1) displays a regular increase in Cu grade with increase in chalcopyrite content and Au and Ag grades, as indicated by the presence of their minerals. The main Ni and Co carrier is pyrrhotite (0.05–0.1 wt % Ni, <0.1 wt % Co); in addition, an Ni

was identified in cobaltite, and Ni and Co, in arsenopyrite. The vanadium content in this ore type is the highest among all ore types; this reflects the wide development of vanadium and vanadium carrier minerals both in the ores proper and in the relics of quartz–albite veinlets enclosed in them (Fig. 5).

Massive pyrite ores (Fig. 7) were recognized as pockets up to 1 m in diameter and thin (up to 50 cm) zones and were exposed in two trenches (Fig. 2). The boundary of these and massive pyrrhotite ores is distinct, without a gradual transition (Fig. 7b). The pyrite ores, like the massive pyrrhotite type II ores, contain the relics of quartz–albite veinlets (Figs. 7c, 7d), which contain Cr–Sc–V mineralization (Kompanchenko et al., 2018).

The pyrite ores are composed of coarse-grained pyrite crystals and their intergrowths (up to several centimeters across); the interstices are filled with pyrrhotite, sphalerite, or chalcopyrite, as well as silicates. The boundaries between pyrite and other sulfides are typically abrupt, without intermediate phases (Fig. 8a). At times hydrous iron oxides, that is, goethite and lepidocrocite, are encountered in fractures along pyrite boundaries.

Pyrite displays high microhardness values (1100–1200 kg/mm^2); etching with the vapor of nitric acid mixed with fluorite powder failed to reveal hidden zoning. Pyrite segregations contain globular porous forms (Figs. 8b, 8c), which are probably the relics of pyrite–marcasite aggregate with a bird's-eye texture. As well, numerous aggregates of equally oriented finely columnar quartz and albite inclusions (Figs. 8d, 8e) were noted in the marginal parts of pyrite crystals. Sphalerite occurs as large nests in the interstices of pyrite crystals or in close intergrowth with pyrite (Figs. 8f, 8g). Sphalerite is characterized by vivid red internal reflex. In addition, sphalerite segregations with fine chalcopyrite and pyrrhotite dissemination, which looks like emulsion dissemination, were encountered. Sphalerite etching demonstrated that the fine chalcopyrite and pyrrhotite dissemination is located at the boundaries of individual sphalerite crystals in an intergrowth. Chalcopyrite and pyrrhotite were encountered as xenomorphic segregations and veinlets between pyrite crystals and as inclusions in pyrite. In addition, galena and hessite were found as small (30 μm) inclusions in pyrite.

Pyrite crystals sometimes contain inclusions that consist of unique assemblages, which are never encountered in other ore types (Figs. 8h–8l). These, for instance, are aggregates of the minerals of crichtonite group (Figs. 8h, 8i); kyzylkumite and rutile intergrowths (Figs. 8i, 8j); or associations of vanadium and vanadium bearing silicates, including unidentified phases, which may prove to be new mineral species as a result of subsequent analysis (Figs. 8k–8l).

The chemical composition of the ores is characterized by elevated Co and Cu grades and a reduced Ni grade (Table 1). The main carrier minerals of these elements are pyrite, chalcopyrite, and pyrrhotite, respectively. Au grades are above average in all ore types, although its carrier minerals were not identified (Table 1). The only silver-carrier mineral identified is rare hessite (Table 2); this agrees with the low silver grade in this ore type. Silver and gold impurities in other minerals are either not found or are below the detection limit. The vanadium distribution trends are similar to those in the massive pyrrhotite type II ores.

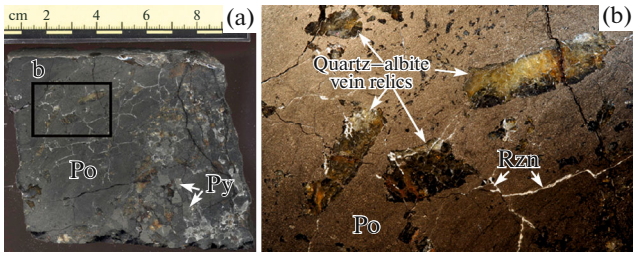

Fig. 5. Type II massive pyrrhotite ore (a) with quartz-albite vein relics (b). Polished sample. Po, pyrrhotite; Py, pyrite; Rzn, rozenite.

DISCUSSION

The extensive pyrrhotitization of massive sulfide ores in the Kola Region, located in the PIV belt, resulted from their deep metamorphic alteration. According to calculated and experimental data (Toulmin and Barton, 1964; Peacock, 1981; Craig and Vokes, 1993; Finch and Tomkins, 2017), the areal extent of pyrite pyrrhotitization and pyrrhotite increases with metamorphic grade. This is typical of the ores not only in the Kola region, but also in Karelia (Rybakov, 1987).

Volcanic-hosted massive sulfide (VHMS) ore transformation stages follow the trend described in the literature. By analogy with other Paleozoic and Recent deposits, we may suggest that pyrite was the primary mineral in massive sulfide ores. As a result of metamorphic transformations, pyrite was replaced by pyrrhotite, and the extent of pyrrhotitization increased with the metamorphic grade. According to arsenopyrite geothermometry data (Scott, 1983; Skott, 1984), the temperature of metamorphism was approximately 490°C. An increase in temperature led to cobalt and nickel redistribution into the disulfide phase. The relative Ni concentration compared to Co is higher in pyrrhotite, while the Co concentration, on the contrary, is higher in pyrite (Bezmen et al., 1975). As a result of a temperature decrease, pyrrhotite was extensively replaced by a pyrite–marcasite aggregate with a bird's-eye texture, which was subsequently replaced by hydrous iron oxides. However, the resumed increase in temperature led to the formation of "metamorphic" pyrite after the pyrite–marcasite aggregate.

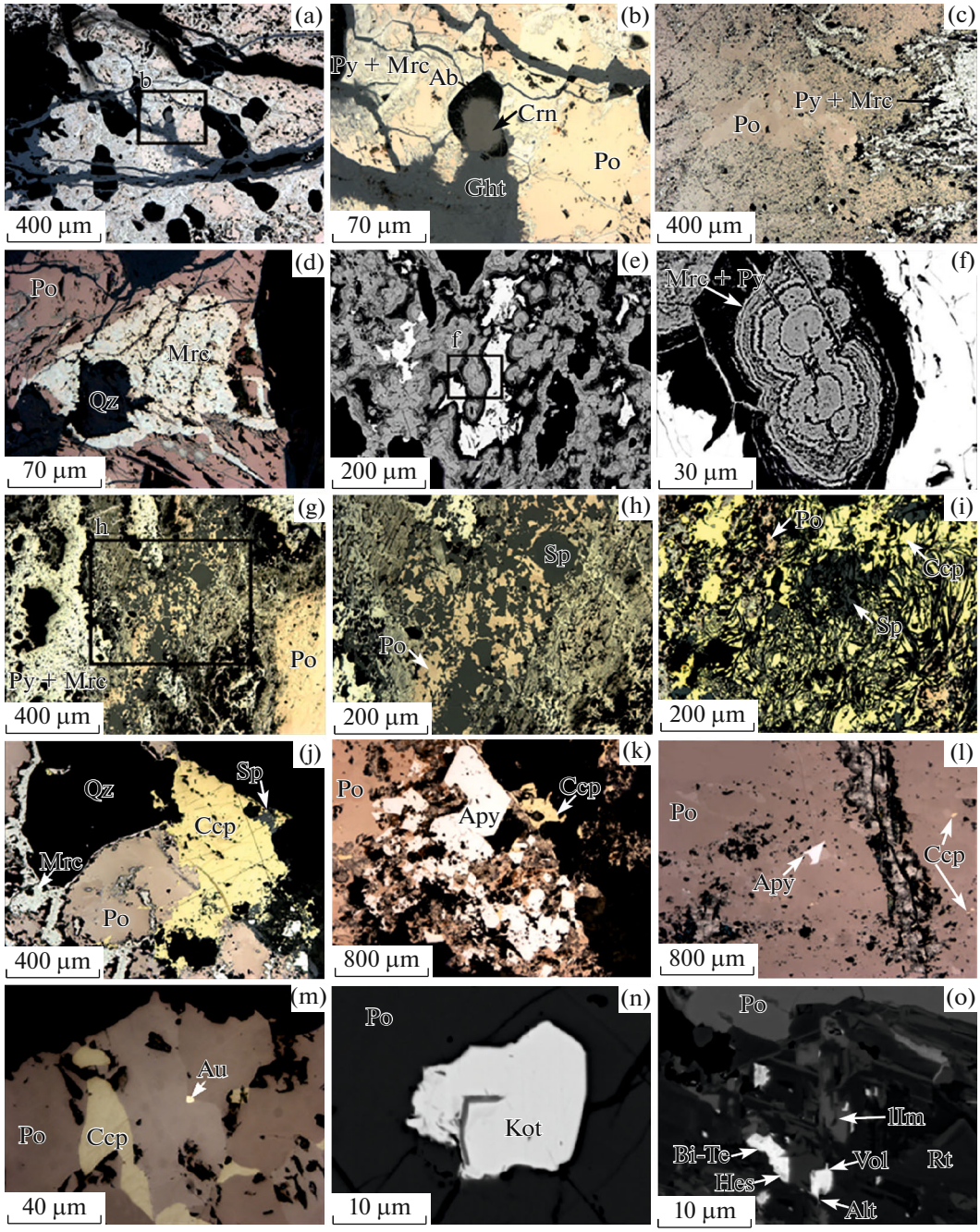

Fig. 6. The major (a–j) and rare (k–o) minerals in type II massive pyrrhotite ores. Backscattered electron (e, f, n, o) and reflected polarized light (the rest) images. Ab, albite; Alt, altaite; Apy, arsenopyrite; Au, native gold; Bi-Te, Bi–Te mineral phase; Ccp, chalcopyrite; Crn, minerals of crichtonite group; Ght, goethite; Hes, hessite; Ilm, ilmenite; Kot, kotulskite; Mrc, marcasite; Po, pyrrhotite; Py, pyrite; Qz, quartz; Rt, rutile; Sp, sphalerite; Vol, volynskite.

The presence of some unique mineral assemblages in massive pyrite ores and their absence in the pyrrhotite ores of both types may indicate the resumption of temperature and pressure increase. As a result, only the assemblages that were captured in the crystals of the "metamorphic" pyrite, which is resistant to external effects, were preserved (Figs. 8i–8l). Kyzylkumite, which is found only inside pyrite crystals in pyrite ores, can provide a sort of temperature benchmark. According to the published data (Smyslova et al., 1981), kyzylkumite transforms to rutile at 320–390°C. As a result of an increase in temperature, kyzylkumite was completely replaced by rutile in pyrrhotite ores and remained intact in pyrite ores.

The massive sulfide ores of the Kola region can be classified as *Cyprus-type* (Dergachev et al., 2010)

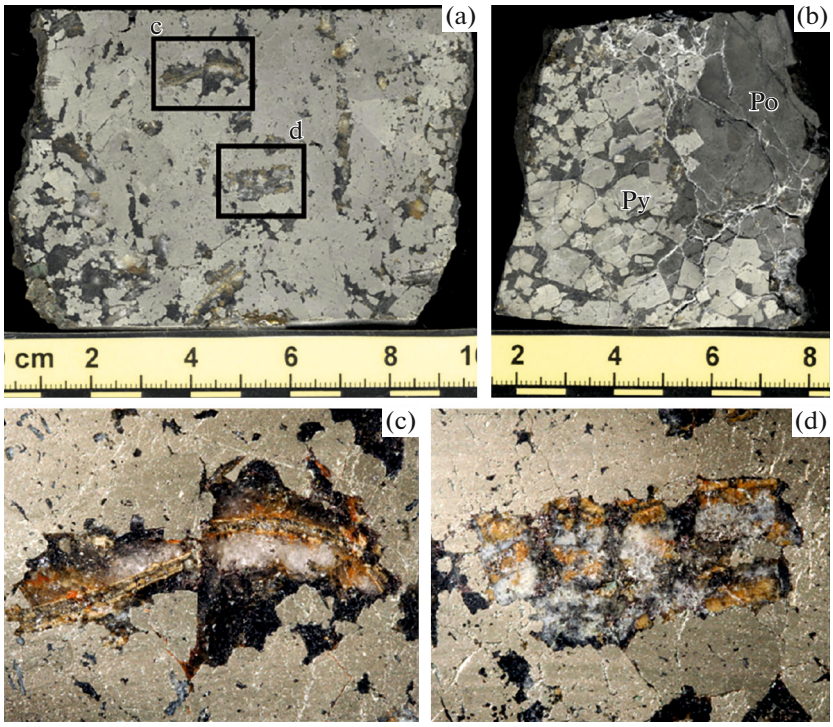

Fig. 7. Massive pyrite ore (a) with quartz–albite vein relics (c, d) and the transitional zone between mPy and mPo-II (b). Polished sections.

based on a number of signatures (low Cu, Ni, and Au reserves; depletion in lead; occurrence in island-arc settings). In terms of the basic characteristics, i.e., geological setting, age, metamorphic grade, and mineral composition, the massive sulfide ores of the Kola region are similar to the known massive sulfide deposits such as Vihanti and Outokumpu (Finland), Sätra (Sweden), and Rampura Agucha (India). These deposits occur within Paleoproterozoic rift belts in host rocks of an island-arc origin. Their age is ca. 1.9 Ga (Rouhunkoski, 1968; Peltola, 1978; Rauhamäki et al., 1980; Gandhi et al., 1984; Deb et al., 1989; Deb, 1992; Allen et al., 1996; Höller and Gandhi, 1997; Peltonen, 2005). Interestingly, the formation of all these deposits coincides with the peak of one of the largest VHMS ore-emplacement outbursts in the Earth's history, 1890–1850 Ma (Dergachev et al., 2010). It is believed that the host rocks and ores underwent metamorphism of amphibolite facies and, as a result, ores composed essentially of pyrrhotite are predominant. In addition, all these ore deposits and occurrences have another feature in common, that is, the development of a unique vanadium mineralization, untypical of Phanerozoic or Recent VMS ores (Long et al., 1963; Zakrzewski et al., 1982; Höller and Stumpfl, 1995; Sergeeva et al., 2011). In spite of this similarity, the massive sulfide ores of the Kola region do not contain mineable concentrations of any valuable components. This can be explained by the primary ore depletion in valuable components; the removal of elements as a result of metamorphism and by hydrothermal solutions; or by insufficient exploration coverage of massive sulfide-ore occurrences.

CONCLUSIONS

1. In terms of rock structure, the ores at the Bragino massive sulfide-ore occurrence are presented by the massive, banded, brecciated, and disseminated varieties. The most widespread type is the massive ores, which are subdivided into three types based on mineral composition: type I massive pyrrhotite ores, type II massive pyrrhotite ores, and pyrite ores. The massive sulfide ores of the Cis-Khibiny structural zone are similar to the massive pyrrhotite type II ores.

2. The major ore minerals are pyrrhotite for the first two types and pyrite, for the third type. Each ore type has a number of typomorphic signatures, including the specific composition of vanadium and vanadium-carrier mineral assemblage.

3. The extensive pyrrhotitization of the ores and the presence of etch-resistant pyrite are signatures of deep metamorphic transformation of the ores.

4. In terms of the basic characteristics, namely, the geological setting, age, the grade of metamorphism, and mineral composition, the massive sulfide ores of the Kola region are similar to the ores of the well known VMS deposits, such as the Vihanti and Outokumpu (Finland), Sätra (Sweden), and Rampura Agucha (India); this makes them potentially important projects.

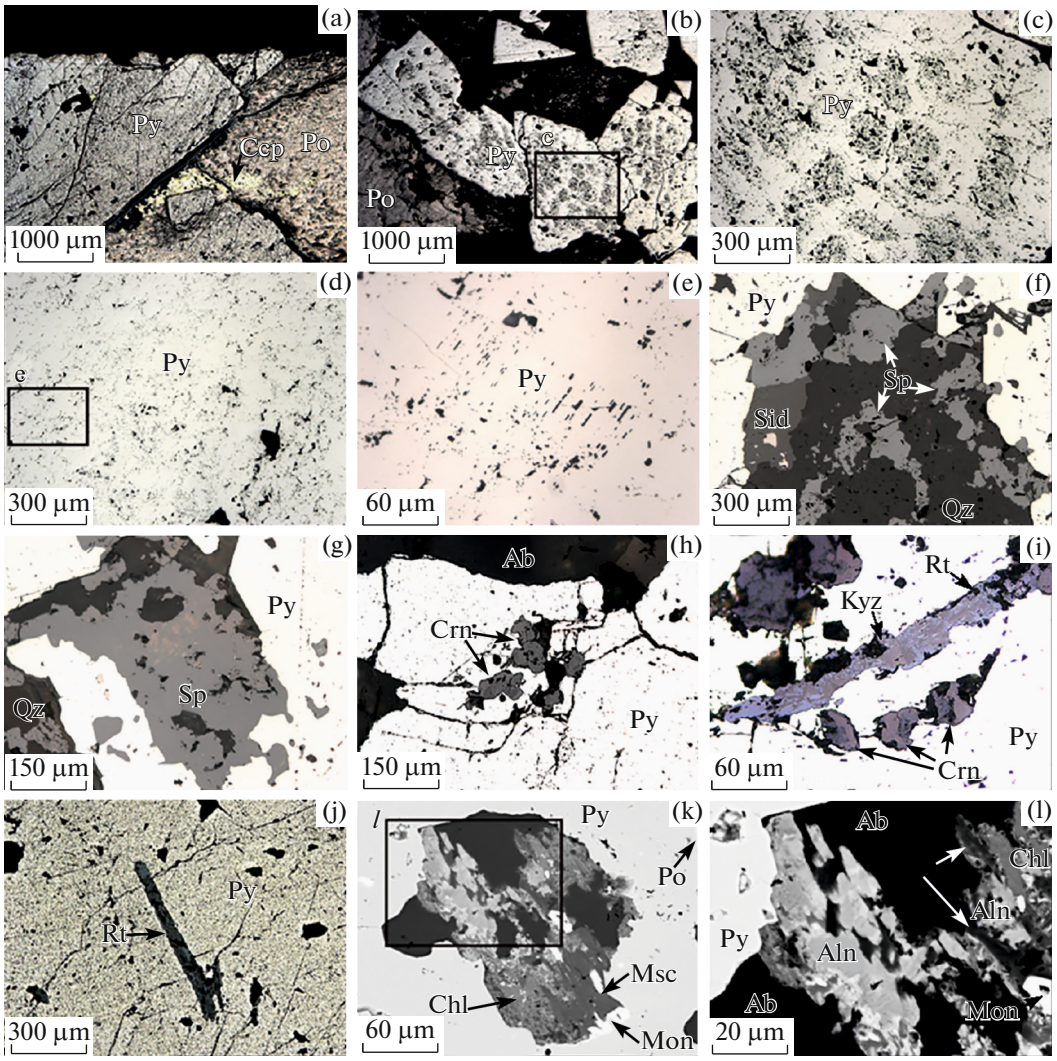

Fig. 8. The major (a–g) and rare (h–l) minerals in massive pyrite ore. Reflected polarized light (a–j) and BSE (k, l) images. Ab, albite; Aln, allanite; Ccp, chalcopyrite; Chl, chlorite; Crn, minerals of the crichtonite group; Kyz, kyzylkumite; Msc, muscovite; Mon, monazite; Po, pyrrhotite; Py, pyrite; Qz, quartz; Rt, rutile; Sid, siderite; Sp, sphalerite.

ACKNOWLEDGMENTS

We thank the analysts of the Geological Institute, L.I. Konstantinova for the analyses of the chemical composition of the ores and A.V. Chernyavskii, for the photographs of the samples. Also, we thank V.V. Shilovskikh and N.S. Vlasenko (Resource Center "Geomodel", Saint Petersburg State University) for helping in minerals investigations and E. Murashova for translating of this article.

REFERENCES

Akhmedov, A.M., Voronyaeva, L.V., Pavlov, V.A., et al., The gold content of the South Pechenga structural zone (Kola Peninsula): types of manifestations and prospects for identifying industrial gold contents, *Regional Geol. Metallogen.*, 2004, no. 20, pp. 143–165.

Allen, R.L., Lunstrom, I., Ripa, M., Simeonov, A., and Christofferson, H., Facies analysis of of a 1.9 Ga, continental margin, back-arc, felsic caldera province with diverse Zn–Pb–Ag–(Cu–Au) sulfide and Fe oxide deposits, Bergslagen Region, Sweden, *Econ. Geol.*, 1996, vol. 91, pp. 979–1008.

Balashov, Y.A., Paleoproterozoic geochronology of the Pechenga–Varzuga structure, Kola Peninsula, *Petrology*, 1996, vol. 4, no. 1, pp. 1–22.

Bezmen, N.I., Tikhomirova, V.I., and Kosogova, V.P., Pyrite-pyrrhotite geothermometer: distribution of nickel and cobalt, *Geokhimiya*, 1975, no. 5, pp. 700–714.

Craig, J.R. and Vokes, F.M., The metamorphism of pyrite and pyritic ores: an overview, *Mineral. Mag.*, 1993, vol. 57, pp. 3–18.

Deb, M., Lithogeochemistry of rocks around Rampura Agucha massive zinc sulfide ore-body, NW India - implications for the evolution of a Proterozoic "Aulacogen", In: *Metallogeny Related to Tectonics of the Proterozoic Mobile Belts*, Sarkar, S.C., Rotterdam: Balkhema, 1992, pp. 1–35.

Deb, M., Thorpe, R.L., Cumming, G.L., and Wagner, P.A., Age, source and stratigraphic implications of Pb isotope data for conformable, sediment-hosted, base metal deposits in the Proterozoic Aravalli-Delhi orogenic belt, northwestern India, *Precambrian Res.*, 1989, vol. 43, pp. 1–22.

Dergachev, A.L., Eremin, N.I., and Sergeeva, N.Ye., Ophiolite-hosted volcanogenic massive sulfide deposits, *Vestn. Mosk. Gos.. Univ., Ser. 4. Geol.*, 2010, no. 5, pp. 3–11.

Finch, E.G. and Tomkins, A.G., Pyrite-pyrhotite stability in a metamorphic aureole: implications for orogenic gold genesis, *Econ. Geol.*, 2017, vol. 112, pp. 661–674.

Gandhi, S.M., Paliwal, H.V., and Bhatnagar, S.N., Geology and ore reserve estimates of Rampura Agucha lead zinc deposit, Bhilwara District, *J. Geol. Soc. India*, 1984, vol. 25, pp. 689–705.

Höller, W. and Stumpfl, E.F., Cr–V oxides from the Rampura Agucha Pb–Zn–(Ag) deposit, Rajasthan, India, *Can. Mineral.*, 1995, vol. 33, pp. 745–752.

Höller, W. and Gandhi, S.M., Origin of tourmaline and oxide minerals from the metamorphosed Rampura Agucha Zn–Pb–(Ag) deposit, Rajasthan, India, *Mineral. Petrol.*, 1997, vol. 60, pp. 99–110.

Karpov, S.M., Voloshin, A.V., Savchenko, Ye.E., and Selivanova, E.A., Vanadium-bearing minerals in ores of the massive sulfide deposite Pyrrhotite Gorge (Khibiny region), *Zap. Ross. Mineral. O-va*, 2013, no. 3, pp. 83–99.

Kompanchenko, A.A., Voloshin, A.V., Bazai, A.V., and Polekhovsky, Yu.S., Evolution of chromium-vanadium mineralization in massive sulfide ores at the Bragino occurrence of South Pechenga structure zone (Kola Region) by example of spinel group minerals, *Zap. Ross. Mineral. O-va*, 2017a, no. 5, pp. 44–58.

Kompanchenko, A.A., Voloshin, A.V., and Sidorov, M.Yu., Minerals of Fe in the oxidation zone of the massive sulfide ore in the South Pechenga structure zone, Kola Region: identification by the Raman spectroscopy, *Vestn. Murmansk. Gos. Tekhn. Univ.*, 2017b, vol. 20, no. 1, pp. 95–103.

Kompanchenko, A.A., Voloshin, A.V., and Balagansky, V.V., Vanadium mineralization in the Kola Region, Fennoscandian Shield, *Minerals*, 2018, vol. 8, p. 474.

Long, J.V.P., Vourelainen, Y., and Kuovo, O., Karelianite, a new vanadium mineral. *Am. Mineral.*, 1963, vol. 48, pp. 33–41.

Melezhik, V.A. and Sturt, B.A., General geology and evolutionary history of the early Proterozoic Polmak–Pasvik–Pechenga–Imandra/Varzuga–Ust'Ponoy Greenstone Belt in the north-eastern Baltic Shield, *Earth Sci. Rev.*, 1994, vol. 36, pp. 205–241.

Mints, M.V., Dokukina, K.A., Konilov, A.N., Philippova, I.B., Zlobin, V.L., Babayants, P.S., Belousova, E.A., Blokh, V.I., Bogina, M.M., Bush, D.A., et al., East European Craton: Early Precambrian History and 3D Models of Deep Crustal Structure, *Geol. Soc. Amer. Spec. Paper.*, 2015, vol. 510.

Mitrofanov, F.P., Balashov, Y.A., and Balagansky, V.V., New geochronological data on lower Precambrian complexes of the Kola Peninsula, *Correlation of Lower Precambrian Formations of the Karelia–Kola Region, USSR and Finland*, Apatity: KSC RA, pp. 12–16.

Peacock, S.M., The systematic of Sulfide Mineralogy in the Regionally Metamorphosed Ammonoosuc Volcanic, *Diss. Master Sci. Earth Planet. Sci.*, 1981.

Peltola, E., Origin of Precambrian copper sulfides of the Outokumpu Disctrict, Finland. *Econ. Geol.*, 1978, vol. 73, pp. 461–477.

Peltonen, P., Ophiolites. In: *Precambrian Geology of Finland—Key to the Evolution of the Fennoscandian Shield*, Lehtinen, M., Nurmi, P.A. Ramo, O.T., Eds., Amsterdam: Elsevier, 2005, pp. 237–277.

Rannii dokembrii Baltiiskogo shchita (Early Precambrian of the Baltic Shield), Glebovitsky, V.A., Ed., St. Petersburg: Nauka, 2005.

Reading the Archive of Earth's Oxygenation. Vol. 1. The Palaeoproterozoic of Fennoscandia as context for the Fennoscandian Arctic Russia—drilling early Earth project, Melezhik, V.A., Prave, A.R., Hanski, E.J., Fallick, A.E., Lepland, A., Kump, L.R., and Srauss, H., Eds., Heidelberg: Springer, 2013.

Rauhamäki, E., Mäkelä, T., and Isomäki, O.-P., Geology of the Vihanti mine. In: *Precambrian ores of Finland. Proc. 26th Int. Geol. Congress. Guide to Excursions 078 A + C*. Part 2. Finland, 1980, vol. 2, pp. 14–24.

Rouhunkoski, P., On the geology and geochemistry of the Vihanti zinc ore deposit, Finland, *Bull. Comm. Geol. Finland*, 1968.

Rybakov, S.I., *Kolchedannoe rudoobrazovanie v rannem dokembrii Baltiiskogo shchita* (Massive Sulfide Ore Generation in Early Precambrian of the Baltic Shield), Leningrad: Nauka, 1987.

Scott, S.D., Chemical behavior of sphalerite and arsenopyrite in hydrothermal and metamorphic environments, *Mineral. Mag.*, 1983, vol. 47, pp. 427–435.

Sergeeva, N.E., Eremin, N.I., and Dergachev, A.L., Vanadium mineralization in ore of the Vihanti massive sulfide base-metal deposit, Finland, *Dokl. Earth Sci.*, 2011, vol. 436, pp. 210–212.

Skuf'in, P.K. and Theart, H.F.J., Geochemical and tectono-magmatic evolution of the volcano-sedimentary rocks of Pechenga and other greenstone fragments within the Kola Greenstone Belt, Russia, *Precambrian Res*, 2005, vol. 141, pp. 1–48.

Skuf'in, P.K., Elizarov, D.V., and Zharkov, V.A., Geological and geochemical pecularities of volcanic of the the South Pechenga structural zone, *Vestn. Murmansk. Gos. Tekhn. Univ.*, 2009, vol. 12, no. 3, pp. 416–435.

Smyslova, I.G., Komkov, A.I., Pavshukov, V.V., and Kuznetsova, N.V., Kyzylkumite V $V_2Ti_3O_9$ –a new mineral from a group of complex vanadium and titanium oxides, *Zap. Ross. Mineral. O-va*, 1981, vol. 110, no.5, pp. 607–612.

Toulmin, P. and Barton, P.B., A thermodynamic study of pyrite and pyrrhotite, *Geochim. Cosmochim. Acta*, 1964, vol. 28, pp. 641–671.

Zakrzewski, M.A., Burke, E.A.J., and Lustenhouwer, W.J., Vourelainenite, a new spinel, and associated minerals from the Stra (Doverstorp) pyrite deposit, central Sweden, *Can. Mineral.*, 1982, vol. 20, pp. 281–290.

Translated by E. Murashova